



Title	Effect of Electromagnetic Stirring on Weld Solidification Structure of Aluminum Alloys (Report I) : Investigation on GTA Weld Metal of Thin Sheet
Author(s)	Matsuda, Fukuhisa; Nakagawa, Hiroji; Nakata, Kazuhiro et al.
Citation	Transactions of JWRI. 1978, 7(1), p. 111-127
Version Type	VoR
URL	<a href="https://doi.org/10.18910/8203">https://doi.org/10.18910/8203</a>
rights	
Note	

*The University of Osaka Institutional Knowledge Archive : OUKA*

<https://ir.library.osaka-u.ac.jp/>

The University of Osaka

# Effect of Electromagnetic Stirring on Weld Solidification

## Structure of Aluminum Alloys (Report I)<sup>†</sup>

### —Investigation on GTA Weld Metal of Thin Sheet—

Fukuhisa MATSUDA\*, Hiroji NAKAGAWA\*\*, Kazuhiro NAKATA\*\*\* and Ritsu AYANI\*\*\*\*

#### Abstract

*In order to make clear the mechanism of grain refinement of weld metal structure by means of stirring of molten metal, GTA bead-on-plate welding without filler metal was performed for thin sheet of aluminum alloy using an electromagnetic stirring process. Then, the effect of the intensity and the frequency of magnetic field, welding speed and welding current on weld solidification structure were investigated. Moreover the contributions of the magnetic stirring to extinction of the porosity and the feathery crystal and to homogeneity of composition were investigated.*

*Main conclusions obtained are as follows; (1) Alternate magnetic field is effective on grain refinement. There is the optimum frequency for grain refinement and the optimum frequency is nearly proportional to welding speed. (2) The strong magnetic field is effective to grain refinement, but there is an upper limit owing to formation of a burnt-through bead. (3) The grain refinement is remarkable in the welding condition where the welding speed is low and the whole weld metal is almost composed of columnar crystals. Therefore, at a high welding speed where equiaxed crystal zone is formed in the weld center, the effect of the magnetic field is little. (4) The magnetic stirring is effective to eliminate the formation of feathery crystal and porosities. (5) The magnetic stirring is effective to homogenize the composition of the weld metal.*

#### 1. Introduction

It is very important to improve the weld solidification structure for the welding of some aluminum alloys, because the mechanical properties strongly depend on the solidification structure in weld metal of aluminum alloys except natural age-hardenable alloys. In addition, it is well known that the improvement of the weld solidification structure is also effective to reduce the formation of solidification cracking and porosities.

As the method for improvement of weld solidification structure, several methods have been proposed and attempted, so far. The addition of alloying element in welding electrode such as Titanium(Ti) and/or Boron(B) is one of the effective methods, but excess addition of these alloys deteriorates the toughness of the weld metal<sup>1)</sup> or in case of some welding methods as GTA, it is difficult to add these alloying elements. Moreover, as another effective methods, some processes have been investigated such as mechanical<sup>2), 3)</sup> and

electromagnetic stirrings<sup>4-7)</sup> and ultrasonic vibration<sup>8), 9)</sup> of molten metal during weld solidification. Among these processes, it is considered that the electromagnetic stirring is one of the most effective methods for the improvement of the weld solidification structure and applications of the electromagnetic stirring to the welding process have been already attempted<sup>10-13)</sup>. Nevertheless, as well as the mechanism of grain refinement during weld solidification, the effects of the intensity and the frequency of the magnetic field and the welding condition have not been clear.

Therefore, in this investigation a GTA bead-on-plate welding without a filler metal has been performed for thin sheets of aluminum alloys using the electromagnetic stirring. Then, the effects of the intensity and the frequency of the magnetic field, welding speed and welding current on the weld solidification structure have been investigated. Moreover some considerations have been discussed on the mechanism of grain refinement in weld metal during solidification. In

<sup>†</sup> Received on March 27, 1978

\* Professor

\*\* Research instructor

\*\*\* Research associate

\*\*\*\* Formerly graduate student, with Sasakura Engineering Co., Ltd.

**Table 1** Chemical composition of materials used

Material	Code	Sheet thickness (mm)	Chemical composition (wt %)									
			Cu	Si	Fe	Mn	Mg	Zn	Cr	Ti	Zr	B
1050	(A)	4	<0.01	0.08	0.25	<0.01	<0.01	<0.01	<0.01	0.02	—	<0.01
1100	(B)	2	0.01	0.14	0.52	<0.01	<0.01	0.01	<0.01	<0.01	—	<0.001
2017	(C)	4	3.80	0.27	0.23	0.45	0.56	0.02	<0.01	0.01	—	<0.01
2024	(D)	2	3.65	0.71	0.30	0.69	0.70	0.31	0.05	0.03	—	<0.001
5052	(E)	2	<0.01	0.08	0.26	0.01	2.54	<0.01	0.18	0.04	—	<0.001
"	(F)	"	0.02	0.08	0.21	0.02	2.76	<0.01	0.33	<0.01	—	<0.01
5083	(G)	2	<0.01	0.09	0.25	0.62	4.38	0.01	0.09	0.04	—	—
"	(H)	"	0.03	0.11	0.24	0.48	4.32	0.02	0.13	0.02	—	<0.01
"	(I)	4	<0.01	0.07	0.17	0.61	4.78	0.02	0.23	<0.01	—	<0.01
"	(J)	2	"	"	"	"	"	"	"	"	"	"
7N01	(K)	2.5	0.08	0.08	0.25	0.35	1.26	4.77	0.20	0.10	0.16	<0.001

addition, the effects of the electromagnetic stirring on the formation of the feathery crystal and porosities and also the homogeneity of composition of the weld metal have been investigated.

## 2. Materials Used and Experimental Procedure

### 2.1 Materials used

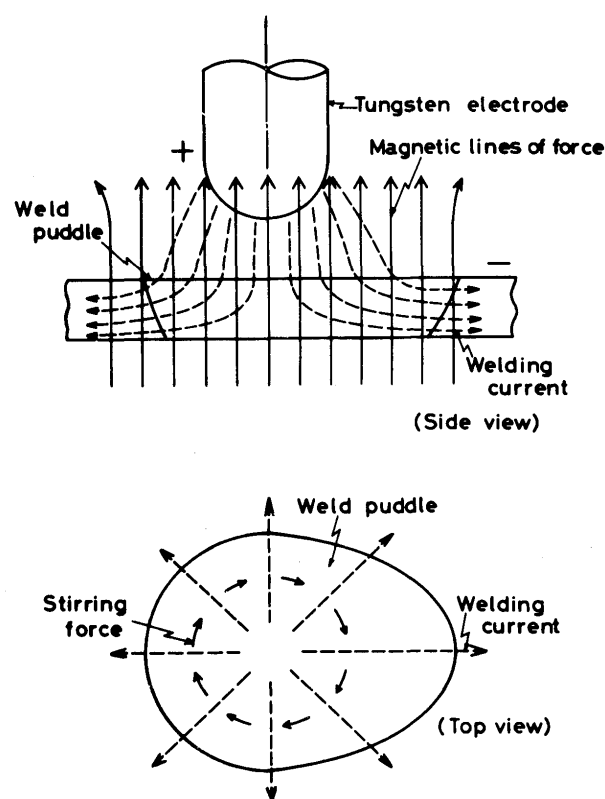
The materials used are commercially pure 1050 and 1100, Aluminum-Copper (Al-Cu) 2017 and 2024, Aluminum-Magnesium (Al-Mg) 5052 and 5083 and Aluminum-Zinc-Magnesium (Al-Zn-Mg) 7N01 alloys. Chemical compositions of these materials used are shown in **Table 1**, the thickness of which are mostly 2 mm, and in 1050, 2017, 5083 (I) and 7N01 (K), are 4 or 2.5 mm.

In order to investigate the difference in the grain refinement in the same type of alloy whose compositions are little different within the range allowed by JIS (Japan Industrial Standard), two or three types of 5052 or 5083 were used, respectively. In addition, 5083 (I) has same compositions of 5083 (J), which was rolled from 4 to 2 mm in thickness so as to examine the effect of the thickness of the specimen on the grain refinement. The dimension of the testing specimen used is 150 mm in length and 100 mm in width.

### 2.2 Experimental procedure

#### 2.2.1 Electromagnetic stirring apparatus

The schematic illustration for the principle of electromagnetic stirring in this investigation is shown in **Fig. 1**. In **Fig. 1**, it is considered that welding current spreads radially from an arc into molten pool (see top view) and passes through it to the direction almost parallel to a sheet surface (see side view). When the magnetic field is applied to the molten pool at the direction perpendicular to the sheet surface during

**Fig. 1** Illustration of principle of electromagnetic stirring

welding, a molten metal in the weld puddle is turned round by Lorentz force induced by the interaction of welding current and magnetic field as shown in **Fig. 1**. Therefore, if an alternate magnetic field is applied, the flow direction of molten metal is periodically changed and then the effect of stirring of molten metal on the improvement of solidification structure will be expected.

The schematic illustration of the arrangement of magnetic coil, welding torch and specimen is shown in **Fig. 2**. An electromagnetic stirring apparatus

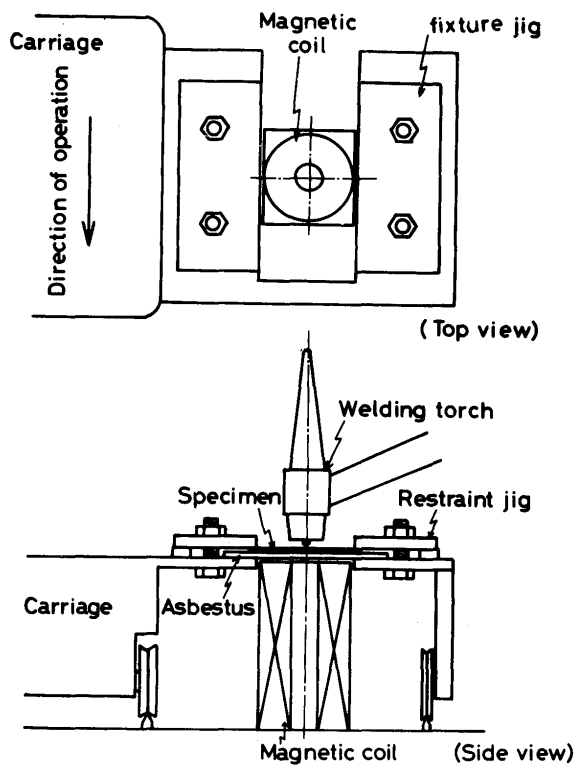


Fig. 2 Arrangement of magnetic coil, welding torch and specimen

consists of a magnetic coil with a ferrous core in center, which was fixed in line with the center of welding torch but under the welding specimen. The specimen can be moved in the preliminary setting speed by an automatic carriage. This arrangement essentially produces a vertical field in the arc and weld zone as shown in Fig. 1. As a power source for the coil, an alternate square wave generator has been used, which can induce a continuous variation of the intensity and the frequency of the magnetic field up to 800 G and from 0.1 to 100 Hz, respectively.

#### 2.2.2 Welding method

GTA (DCRP) bead-on-plate welding without the filler metal has been carried out with a distance of 2 mm between the electrode and the specimen. Pure Ar gas was usually used for shielding and a Ar+H<sub>2</sub> mixing gas with 2% H<sub>2</sub> gas was also used in order to examine the formation of the porosity. A flow rate of the shielding gas was 18 liters/min in each case. The welding speed was changed from 65 to 1000 mm/min and the optimum welding current for each specimen was selected such that a full-penetrated weld bead whose width of both sides were kept almost 8 mm could be obtained under the given welding speed. In such a full-penetrated weld bead, solidification

phenomena such as the growth mode of columnar crystals are considered to be two-dimensional. These welding conditions are listed in Table 2(a). Moreover, the welding conditions shown in Table 2(b) were

Table 2 Welding conditions

Sheet thickness (mm)	Welding speed (mm/min)	Welding current (A)	Bead width (mm)
a	2	65	8
		130	"
		250	"
		500	"
		1000	"
	2.5	250	"
		500	"
		1000	"
	4	130	"
	b	130	7~17
		250	"
		40~70	"
b	2	50~100	"
	4	80~160	"

also used in order to examine the effect of welding current on the grain refinement.

#### 2.2.3 Sham experiment for electromagnetic stirring by using mercury bath

In order to obtain the quantitative recognition about the flow pattern in the weld puddle induced by the electromagnetic stirring, the following experiment has been carried out. At first, the mercury bathes with three different shapes were made as a model of the weld puddle as shown in Fig. 3. A side wall of

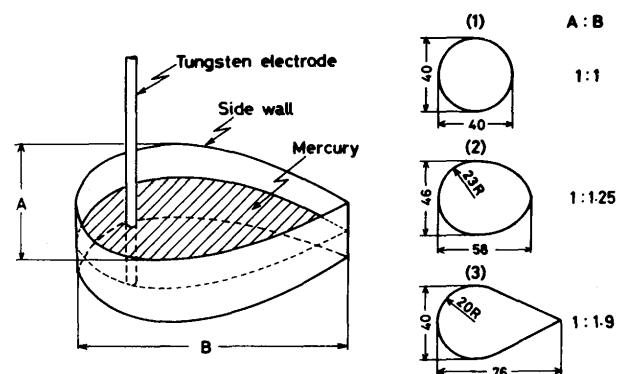


Fig. 3 Shape and dimension of mercury bath

the mercury bath is made of the steel and a bottom of it is made of the plastic.

The surface of the mercury bath was covered with 25% HCl water solution for the protection of the mercury from the oxidation and the fine particles of

SiC was floated on the surface of the mercury bath in order to make clear the flow pattern. Then the magnetic coil was set under the mercury bath and a tungsten electrode (3 mm dia.) was immersed into it. For the observation of the flow pattern, a direct current was passed through the mercury bath from the tungsten electrode to the steel side wall with the alternate magnetic field.

### 3. Experimental Result and Discussion

#### 3.1 Effect of electromagnetic stirring on grain refinement

##### 3.1.1 Effect of location of electric ground

The distribution of welding current in the weld puddle is considered to be affected by the ground position, so that the ground position will affect indirectly on the grain refinement because the degree of the electromagnetic stirring is proportional to the current density.

Figure 4 shows a variation of the macrostructure in the weld metal of 5052 (E) against the ground position. In this case, the intensity and the frequency of the magnetic field were set to the optimum values mentioned in the latter. In Fig. 4, marks of A, B, C, D and E mean the arrangement of the ground position as shown in the schematic diagram. In the case of mark

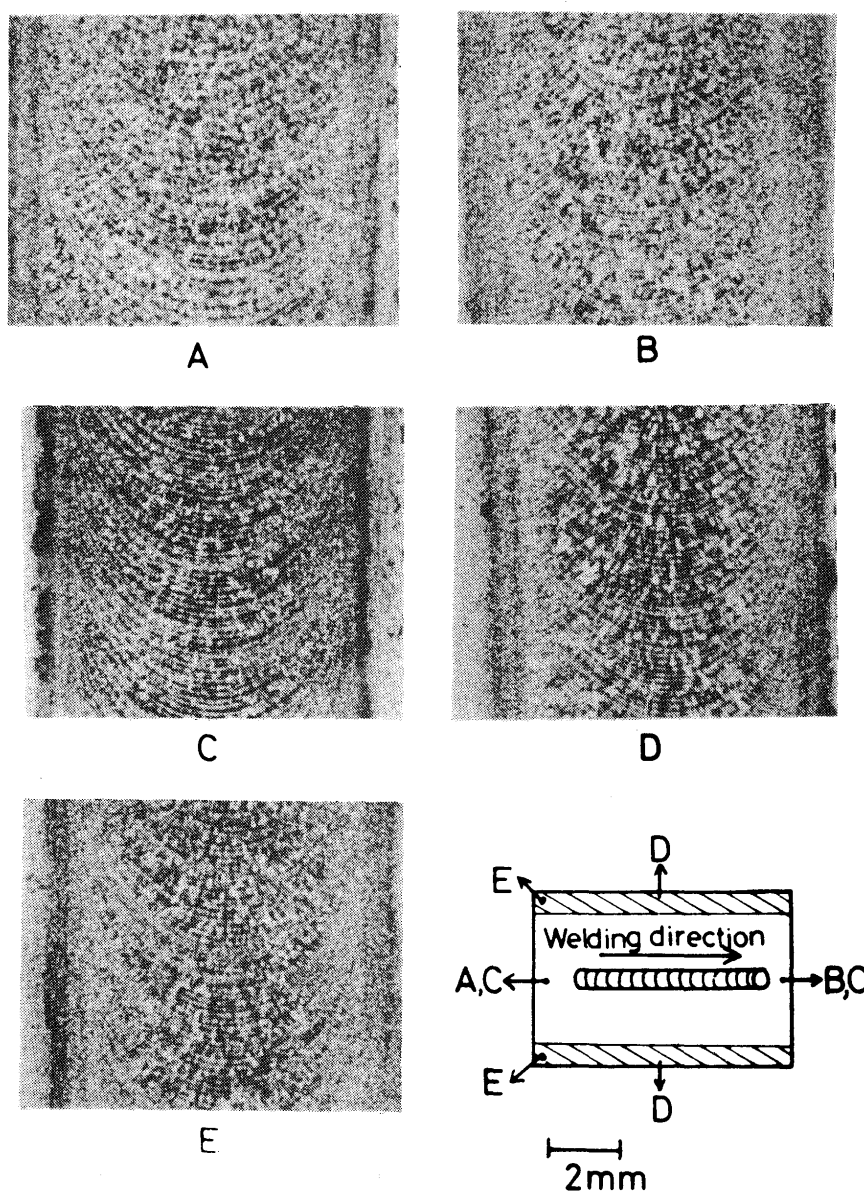


Fig. 4 Effect of ground position on grain refinement. material; 5052(E), welding speed  $V=250$  mm/min, welding current  $I=70$  A, magnetic field; 300G, frequency; 10 Hz

A a ground position was set at the end of the specimen near the arc start, in C the ground was set in both sides of the specimen and in D the ground was set at the shaded portion in both sides of the specimen. As regards to the cases of A, B and C, the grains are remarkably refined throughout the weld bead, but in the cases of D and E, they are refined only in the area near fusion boundaries in the weld bead.

It is considered that the magnetic stirring is more effective in the case of A than B because the magnetic stirring of the molten metal near a solidification front seems to be the most effective to the grain refinement hence in the case of A, the current density at this solidification front of the weld puddle is the largest in all cases. However the experimental results were contrary to the authors expectations.

Judging from these results, it seems that the differ-

ence in the electric conductivity between liquid and solid, the dependence of electric conductivity against temperature, the temperature distribution around the arc and the dimension of the specimen also affect on the current distribution in the weld puddle besides the ground position.

It has been made clear in the above that the ground position largely affected on the grain refinement. Therefore, the ground position was set as well as the case of A in the latter section in this investigation.

### 3.1.2 Effect of frequency of magnetic field

The macrostructure of the weld metal of 5052 (E) is shown in **Fig. 5** where the frequency of the magnetic field was varied to 20 Hz under the constant magnetic field of 300 G. For the unstirred condition the macrostructure consists of the epitaxially grown columnar crystals near fusion boundaries, slender columnar

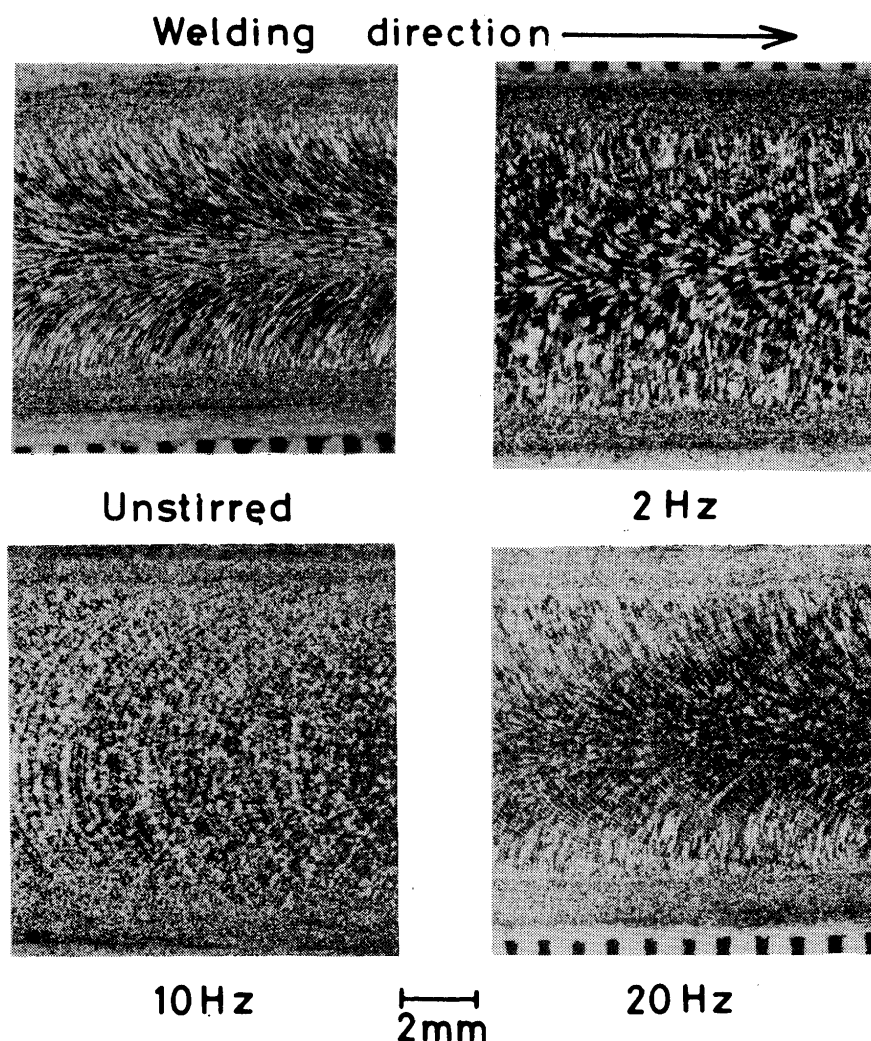


**Fig. 5** Effect of frequency of magnetic field on grain refinement. material; 5052(E),  $V=250$  mm/min,  $I=70$  A, 300G

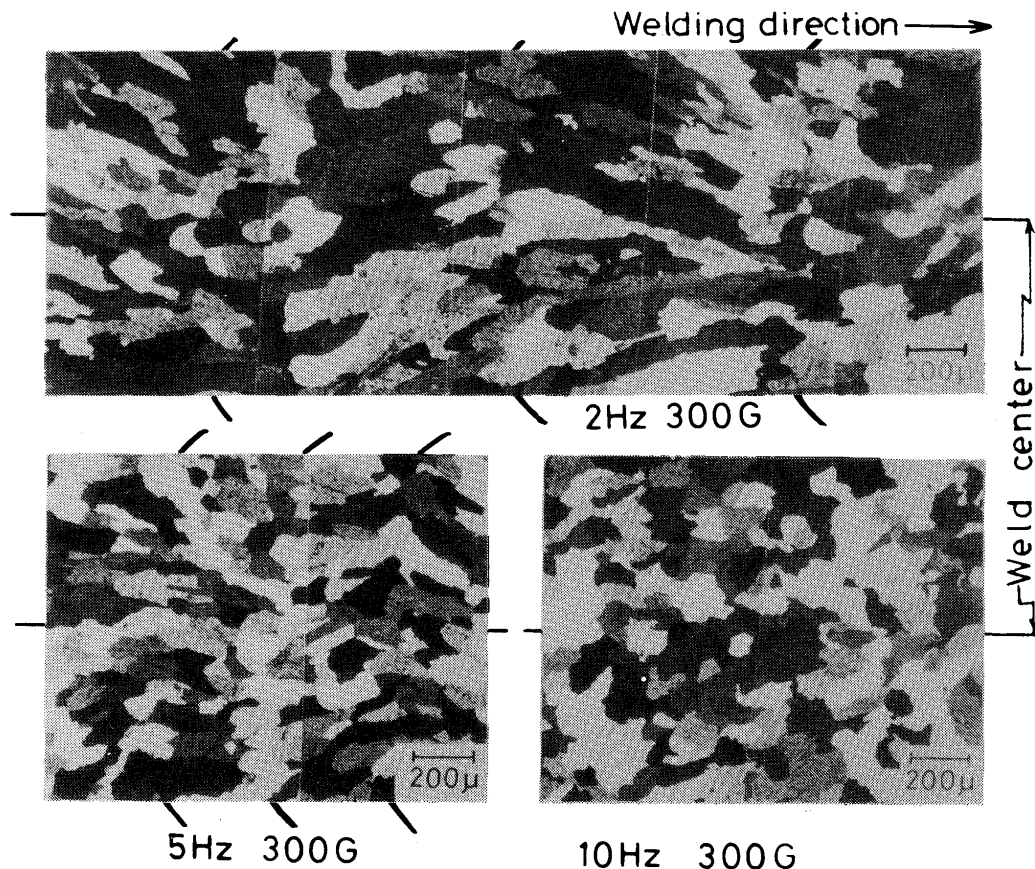


Fig. 6 Effect of frequency of magnetic field on growth period of columnar crystal in weld center. material; 5052(E),  $V=250$  mm/min,  $I=70$  A, 300G

crystals, that is stray crystals<sup>14),15)</sup> in the next middle zones and a little amount of the equiaxed crystals in the central zone of the weld bead.

In the case of 2 Hz, individual stray crystal is decreased in its length in comparison with that unstirred but the grain refinement is not so remarkable. When the frequency of the magnetic field is increased to 10 Hz, the macrostructure is remarkably refined throughout the weld bead. In the case of 20 Hz, however, macrostructure is almost same as well as those unstirred. From these results, it is apparent that there is an optimum in the frequency of the magnetic field for the grain refinement.

Figure 6 shows the microstructure in the weld center along welding direction with the frequencies of 2, 5 and 10 Hz under the same welding condition and the intensity of 300 G as in Fig. 5. Each pair of bold line in the top and bottom of photograph indicated each ripple line where the polarity of the magnetic field was altered. In Fig. 6, in the case of 2 Hz, columnar crystals were periodically altered their di-

rections of growth on the ripple line. The length of the columnar crystal was almost corresponded to the distance between ripple lines. Next, in the case of 5 Hz, the zigzag growth of the columnar crystal was also observed but the length of it became shorter as the distance of ripple line did due to higher frequency. Thus, the grain refinement was the most remarkable in the case of 10 Hz when the distance of ripple line is nearly equal to the width of the columnar crystal, so the solidification structure looks like complete equiaxed crystal in the whole weld bead.

The zigzag growth of the columnar crystal observed in 2 and 5 Hz is due to the formation of new columnar crystals, namely new stray crystal, at the ripple line and not due to the periodical change of the growth direction of  $\langle 100 \rangle$  in individual columnar crystal in every half period of the alternate magnetic field\*\*\*\*. Moreover, the more careful observation for the formation of the new crystal at the ripple line has been carried out and its result is shown in Fig. 7. A pair of bold line in Fig. 7 indicates a ripple line. In Fig.

\*\*\*\* As for the material possessing low susceptibility for the grain refinement such as 1050, it was observed as shown in Fig. 14 that individual columnar crystal was changed its growth direction at every ripple line.





Fig. 7 Occurrence of new crystals at ripple site. material; 5052(E),  $V=250$  mm/min,  $I=70$  A, 400G, 2 Hz

7, many new crystals were originated on a ripple line and then several crystals of those were grown forward (upwards of Fig. 7). On the contrary, most of the columnar crystals reached to this ripple line were suppressed their growth by those new initiated crystals. From these results, it is considered that an alternate change of the flow direction of the molten metal is effective to the grain refinement.

Next, the effect of an unidirectional flow of the molten metal to the grain refinement was investigated by using a constant polarity of the magnetic field. As a result, the grain refinement has not been observed in all of the materials used except 7N01, which is very susceptible for the grain refinement. For an example, in Fig. 8 of 5052 (E), the columnar crystals didn't be

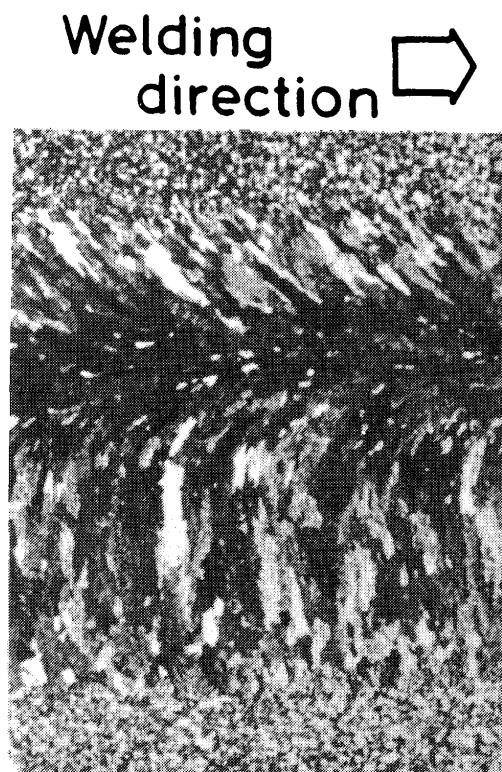


Fig. 8 Effect of steady magnetic field on grain refinement. material; 5052(E),  $V=250$  mm/min,  $I=70$  A, 400G

refined but only grown to a opposite direction of the flow of molten metal even in a strong intensity of the magnetic field as 400 G. This also suggests an importance of the alternate magnetic field for the grain refinement.

Moreover, if the grain refinement is achieved by the mechanism that the length of the columnar crystal is corresponded to a half period of the alternate magnetic field as shown in Fig. 6, the optimum frequency of the alternate magnetic field is considered to be proportional to welding speed since the distance where the columnar crystal can grow in a half period of the alternate magnetic field is proportional to the welding speed. The relation between the welding speed and the optimum frequency is shown in Fig. 9, where macrostructures are shown for various frequencies in the welding speeds of 65, 130 and 250 mm/min. The intensity of the magnetic field is a constant value of 700 G in the welding speeds of 65 and 130 mm/min, of 300 G in that of 250 mm/min. These intensities of the magnetic field were the maximum values respectively to form a stable weld bead because much intensity forms a burnt-through weld bead. In Fig. 9, the optimum frequency for the remarkable grain refinement throughout the weld bead is 2, 5 and 10 Hz in the welding speeds of 65, 130 and 250 mm/min, respectively. Consequently, the optimum frequency is almost proportional to welding speed.

On the other hand, in the case of high welding speed, the optimum frequency could not be found out because the equiaxed crystal was formed near the weld center even in the unstirred weld bead. Therefore, there is no obvious effect for the grain refinement by the magnetic stirring operation in the weld metal of high welding speed.

### 3.1.3 Effect of intensity of magnetic field

The variation of the macrostructures in the weld bead of 5052 (E) is shown in Fig. 10 for various intensities of the magnetic field with 10 Hz of frequency. At first, in the case of 100 G, the structures in the weld metal were remarkably refined near fusion boundaries but not so remarkable near the weld center. Next, increasing the intensity to 300 G, the structures were completely refined all over the weld bead. In excess intensity more than 300 G, however, the weld bead was burnt-through.

Consequently, the strong magnetic field is effective to the grain refinement, but there is an upper limit owing to the formation of the burnt-through weld bead. This upper limit became lowered in the slow welding speed and/or the high welding current.

### 3.1.4 Effect of welding speed



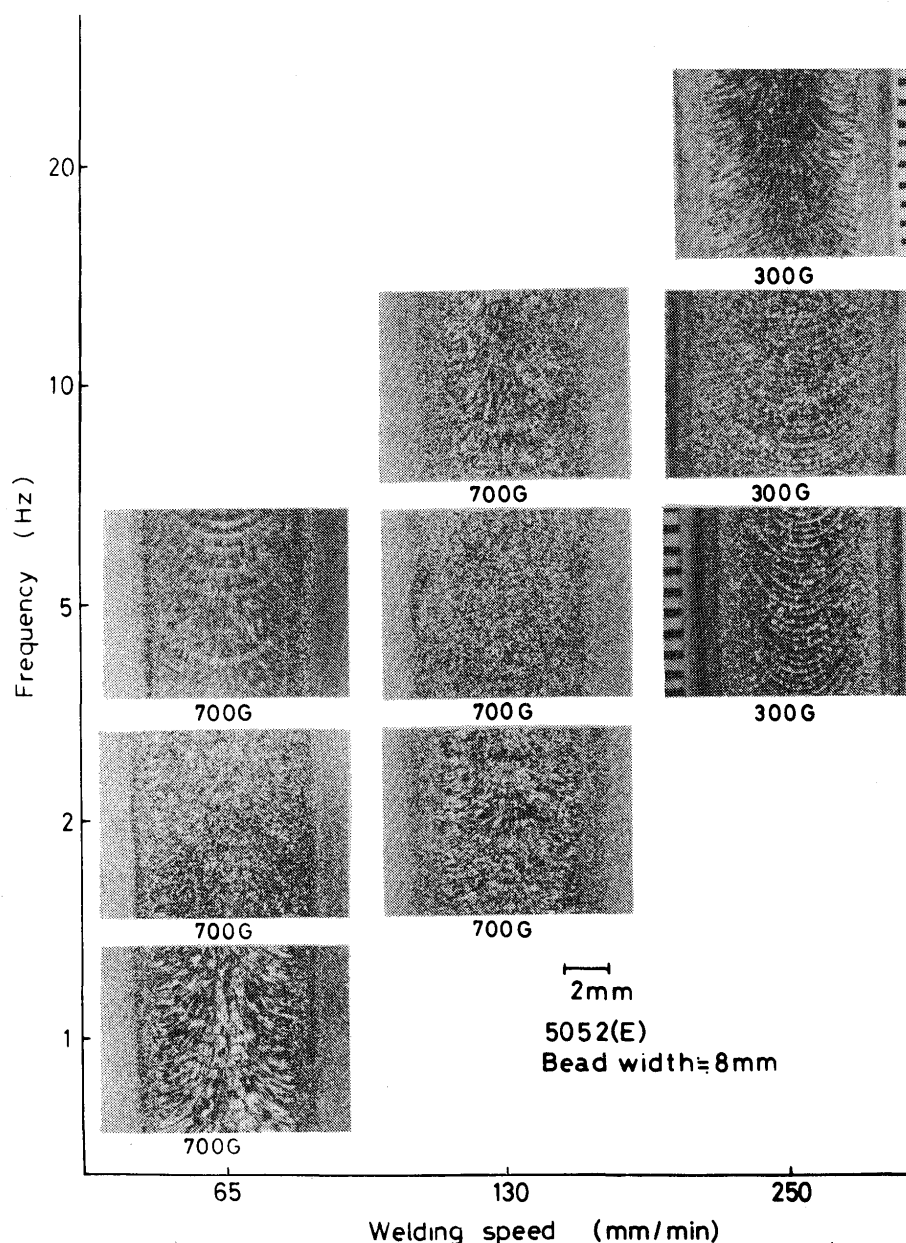


Fig. 9 Dependence of optimum frequency of magnetic field on welding speed. material; 5052 (E)

The macrostructures in the weld metal with and without magnetic field are shown in **Fig. 11** for the welding speeds of 250, 500 and 1000 mm/min. The intensity of the magnetic field was decided so that the product of the welding current and the intensity of the magnetic field was equal to 21,000 because Lorentz force is considered to be equal in each welding speed. The frequency was a constant value of 10 Hz.

At the welding speed of 250 mm/min, the grain refinement is remarkable as previously mentioned. On the other hand, in the welding speeds of 500 and 1000 mm/min, without stirring, the equiaxed crystals

were formed in the weld center zone because of increasing the constitutional supercooling<sup>18)</sup> and then, even when the maximum intensity of the magnetic field was induced, there was no remarkable difference in the macrostructures in comparison with those unstirred, though the grain refinement was observed at ripple lines only near fusion boundaries.

Consequently, it is apparent that the high welding speed decreases the effect of the magnetic field on the grain refinement. This will be due to the teardrop shape of the weld puddle where the molten metal becomes difficult to flow near the solidification front.

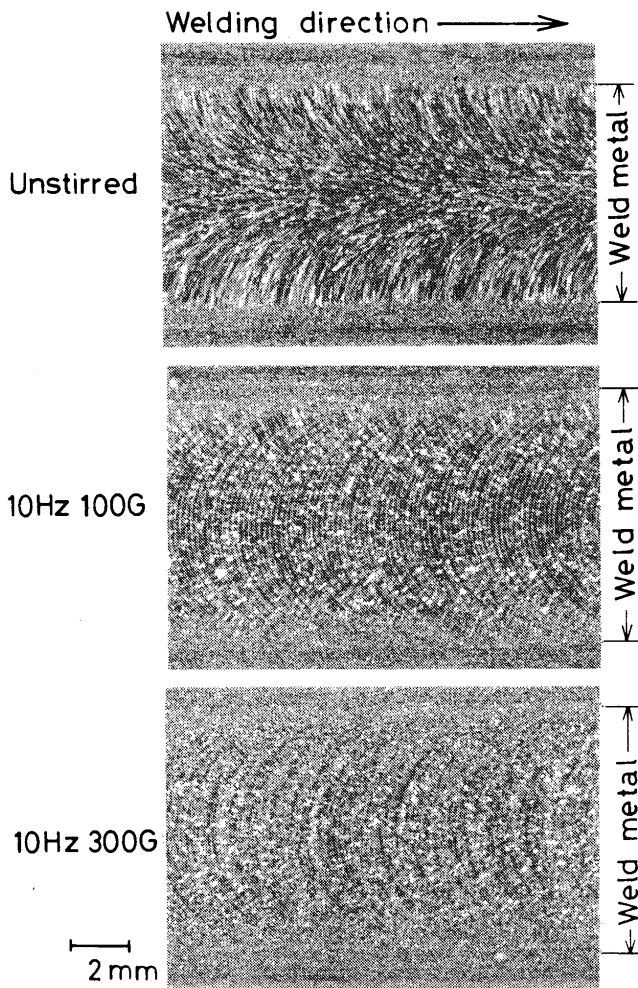


**Fig. 10** Effect of intensity of magnetic field on grain refinement. material; 5052(E),  $V=250$  mm/min,  $I=70$  A, 10 Hz

### 3.1.5 Effect of welding current

An increase in welding current is effective to grain refinement, but there is a limit in maximum owing to the formation of the burnt-through bead. **Figure 12** shows the effect of the welding current and magnetic field on the grain refinement in the weld metal of 5052 (E) under the constant of the welding speed of 250 mm/min and the frequency of 10 Hz. In **Fig. 12** the parameter  $Y$  in percent represents the relative position in the weld bead which indicates the fusion boundary and the center of weld bead for 0 (%) and 100 (%), respectively. In this figure the value of  $Y$  also means that the grain refinement is fully achieved in the range from fusion boundary to the location of  $Y$ .

In **Fig. 12**, in the lower welding current and/or the weak magnetic field, the  $Y$  was smaller than 50% and the grain refinement was not sufficient. On the other hand, in the higher welding current and/or the strong magnetic field the burnt-through bead was

formed. Thus, in the middle of those ranges, the grains were apparently refined. Especially, in the range shaded by the double hatchings, the grains were remarkably refined all over the weld bead, though the range was very narrow.

As regards to the weld solidification structure shown in **Fig. 12**, when the welding current was more than 77 amp, the equiaxed crystal zone was formed near the weld center. On the contrary, when the welding current was less than 77 amp, the structure almost consisted of the columnar crystal. Therefore, the effective range for the grain refinement is restricted to that where the equiaxed crystal zone is not formed without electromagnetic stirring. Moreover, the condition where the grain refinement is achieved all over the weld bead can be obtained by the combination of the maximum welding current where the equiaxed crystal zone is not formed and the maximum intensity of the magnetic field where the burnt-through weld bead is not formed.

As for Lorentz force, if the product of the welding current and the intensity of the magnetic field is a constant value, the degree of the grain refinement is considered to be equal. Therefore, each boundary curve in **Fig. 12** should be essentially drawn as a hyperbolic curve but they didn't so. The reason in the above is considered that the variation in welding current causes the difference in the factors which may be affected to the formation in the melt, such as, the shape and the mass of the weld puddle, the morphology of the cellular dendrite, the temperature distribution on the solidification interface and also arc force and magnetic field due to the welding current itself.

### 3.1.6 Effect of specimen thickness

When the welding current is increased in the two-dimensional weld bead so that the current density in an unit thickness become equal even in different plate thickness, the refinement of the grains will be considered to be same for each other. Therefore the difference in the grain refinement has been investigated in the same welding current by using 5083 (I) and 5083 (J), the thickness of which are 4 and 2 mm, respectively, but the compositions of them are the same in actual.

The macrostructures are shown in **Fig. 13** where the welding current in 5083 (I) is two times as large as in 5083 (J) but the welding speed and the intensity of the magnetic field are the same, that is, 130 mm/min and 700 G, respectively. From comparing **Fig. 13** (a) with (b), even in same magnetic field, the grain refinement was completely achieved all over the weld bead in 4 mm thick sheet but was only observed near

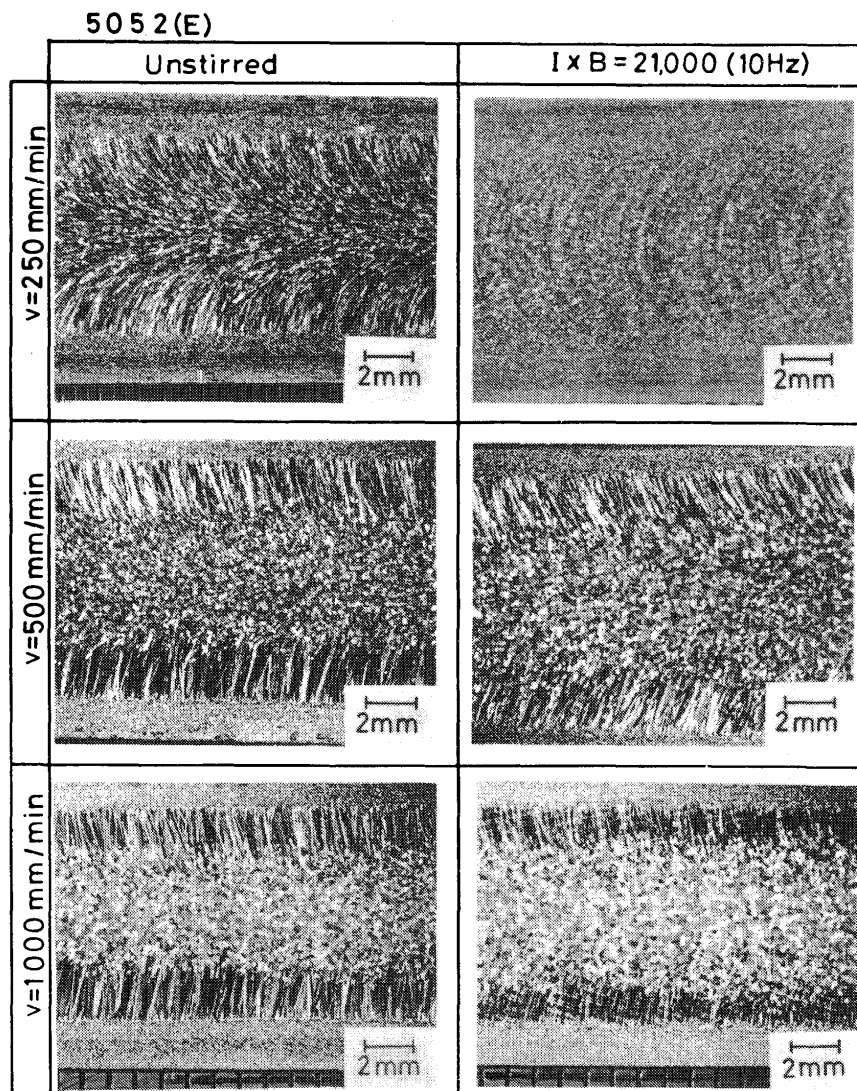


Fig. 11 Effect of welding speed on grain refinement. material; 5052(E), 10 Hz

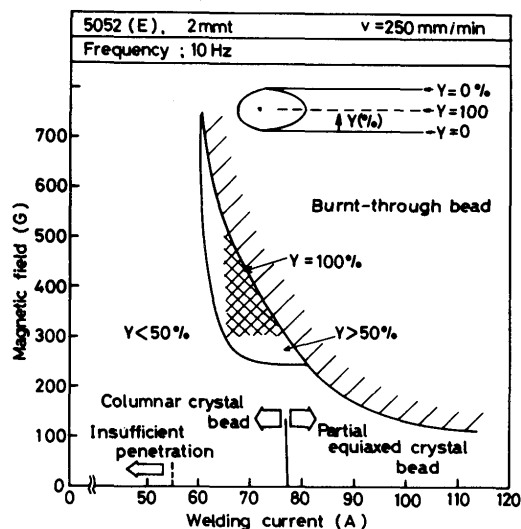


Fig. 12 Composite effect of welding current and intensity of magnetic field on grain refinement. material; 5052(E),  $V = 250$  mm/min, 10 Hz (Number in percent as Y shows the range of equiaxed zone in the weld metal)

the fusion boundaries in 2 mm thick sheet. As a result, even if the current density in a unit thickness is the same in each other, the degree of the grain refinement is not always the same when the thickness of specimen is different. In the above case, it seems that the magnetic field which is induced by the arc and/or the welding current itself may affect the motion of the molten metal during welding.

### 3.1.7 Effect of Material compositions

The effect of the magnetic stirring has largely depended on compositions of material. For a example, the macrostructure of 7N01 (K) consists of large columnar crystals under unstirred condition but it is remarkably refined by the magnetic stirring even with an unidirectional magnetic field. Therefore the optimum zone of the welding parameters and the magnetic field which is effective for the grain refinement is

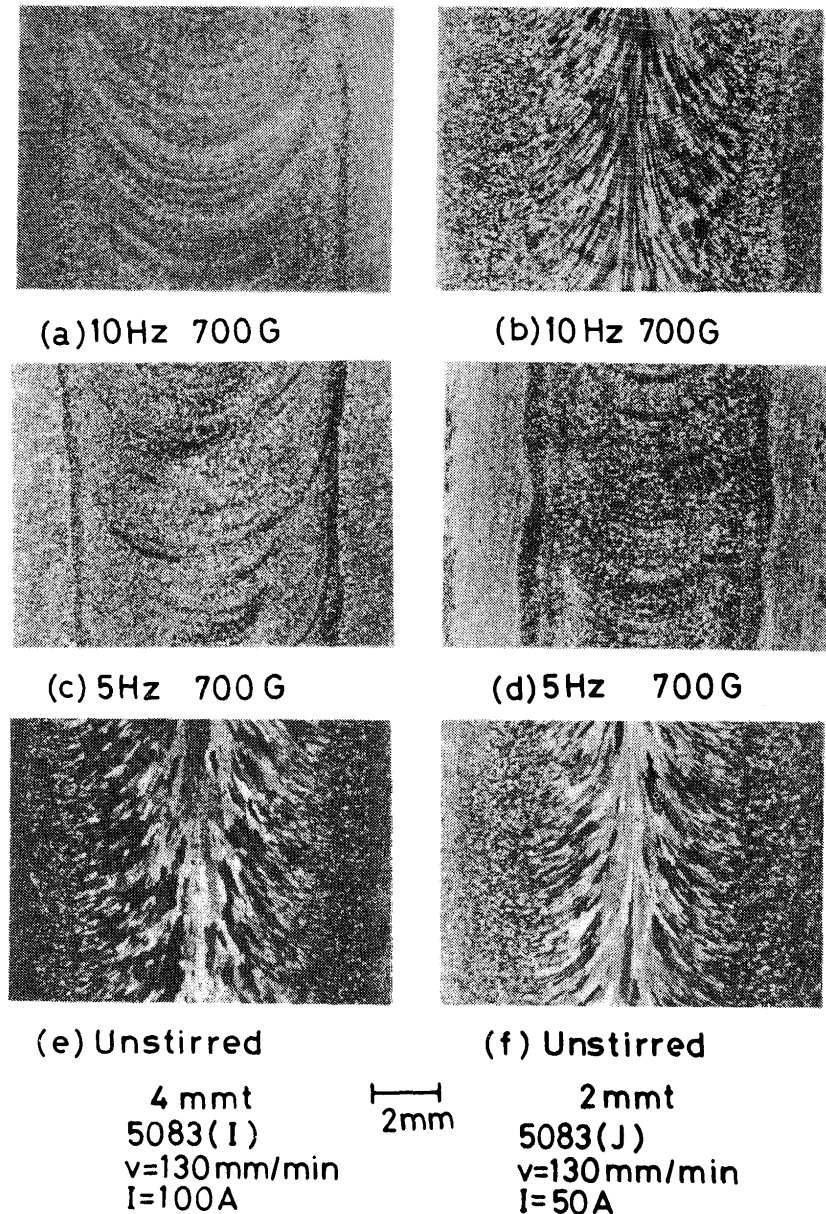


Fig. 13 Effect of sheet thickness on grain refinement. material; 5083(I) and 5083(J)

wider in 7N01 (K). On the contrary, 1050 (A), 1100 (B), 2017 (C) and 2024 (D) are less susceptible for the grain refinement as shown in Fig. 14 which shows the macrostructures in the weld center of 1100 (B) and 2024 (D). The welding condition was the equal to the one where the structure of 5052 (E) were fully refined throughout the weld bead. In Fig. 14, Only the zigzag growth mode of the columnar crystal is observed and the nucleation of the stray crystal at the ripple lines, as observed in Fig. 6, is rare. Moreover, the structures of the weld metals of 1050 (A) and 1100 (B) could not be refined in any condition in this investigation, but those of 2017 (C) and 2024 (D)

could be refined only in the welding speed slower than 130 mm/min.

Meanwhile, a large difference has been observed on the degree of the grain refinement even in the same type of aluminum alloy, such as 5052 or 5083 whose compositions are both satisfied in the JIS Standard. As examples, Fig. 15 shows the comparison of the macrostructure of 5052 (E) with that of 5052 (F) in the same welding and magnetic field condition. The structure of 5052 (E) was remarkably refined by electromagnetic stirring but that of 5052 (F) was rarely refined except near the fusion boundaries. As for the structure without stirring, a number of the small

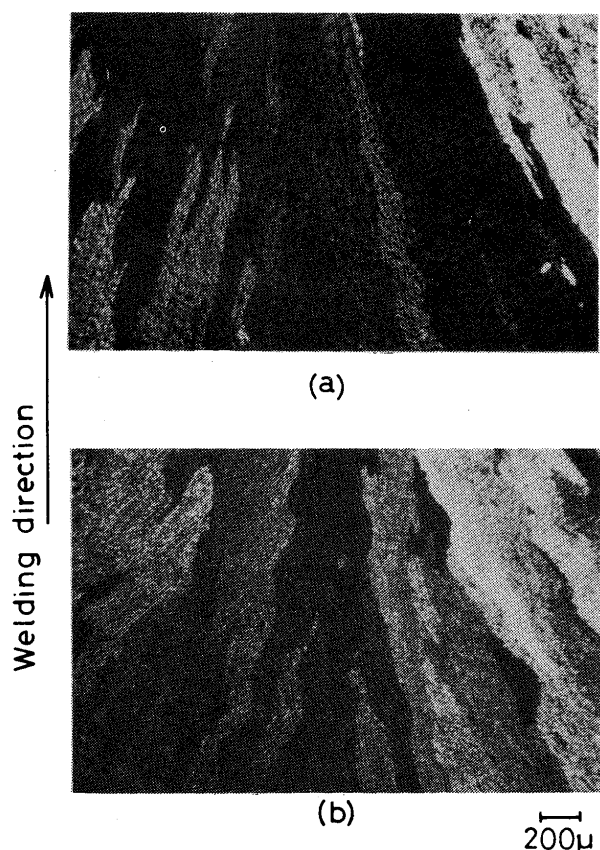


Fig. 14 Effect of electromagnetic stirring on grain refinement of 1100(B) and 2024(D).  $V=250$  mm/min,  $I=70$  A, 10 Hz, 300G (a) 1100(B) (b) 2024(D)

stray crystals are formed and the equiaxed crystals are also partly seen in the weld center in case of 5052 (E). On the contrary, in 5052 (F), the stray crystals were much wider and longer in the weld metal than those in 5052 (E) and the equiaxed crystals were rarely observed in the center. In addition, as regards to 5083 (G) and 5083 (H), the same phenomenon was observed, that is, 5083 (H) whose structure consisted of a number of stray crystals was much susceptible for the grain refinement than 5083 (G). The difference in the structure in the above is well explained by the content of Ti which is well known as a grain refinement element. 5052 (E) and 5083 (G) have more Ti content of 0.04% than 5052 (F) and 5083 (H).

The materials used in this experiment were arranged as follows in order of the susceptibility of the grain refinement: 7N01 (K) > 5052 (E)  $\cong$  5083 (G) > 5052 (F)  $\cong$  5083 (H)  $\cong$  2017 (C)  $\cong$  2024 (D) > 1100 (B)  $\cong$  1050 (A). It is generally considered that the alloy which has the wide solidification range is more susceptible for the grain refinement even if the grain refinement by the electromagnetic stirring is due to the fragmentation of the arms of the cellular dendrite or the nucleation owing to an increase of the constitutional supercooling. As for the nominal solidification range<sup>17), 18)</sup>

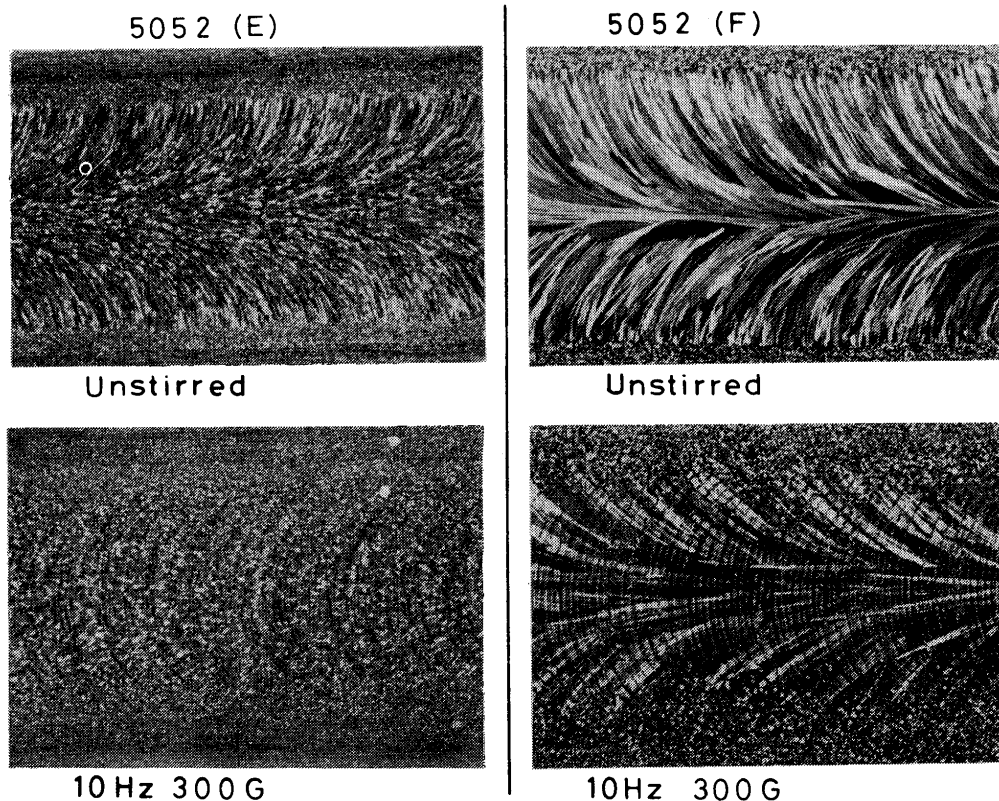


Fig. 15 Difference in grain refinement between materials of same designation in JIS. material; 5052(E) and 5052 (F),  $V=250$  mm/min,  $I=70$  A



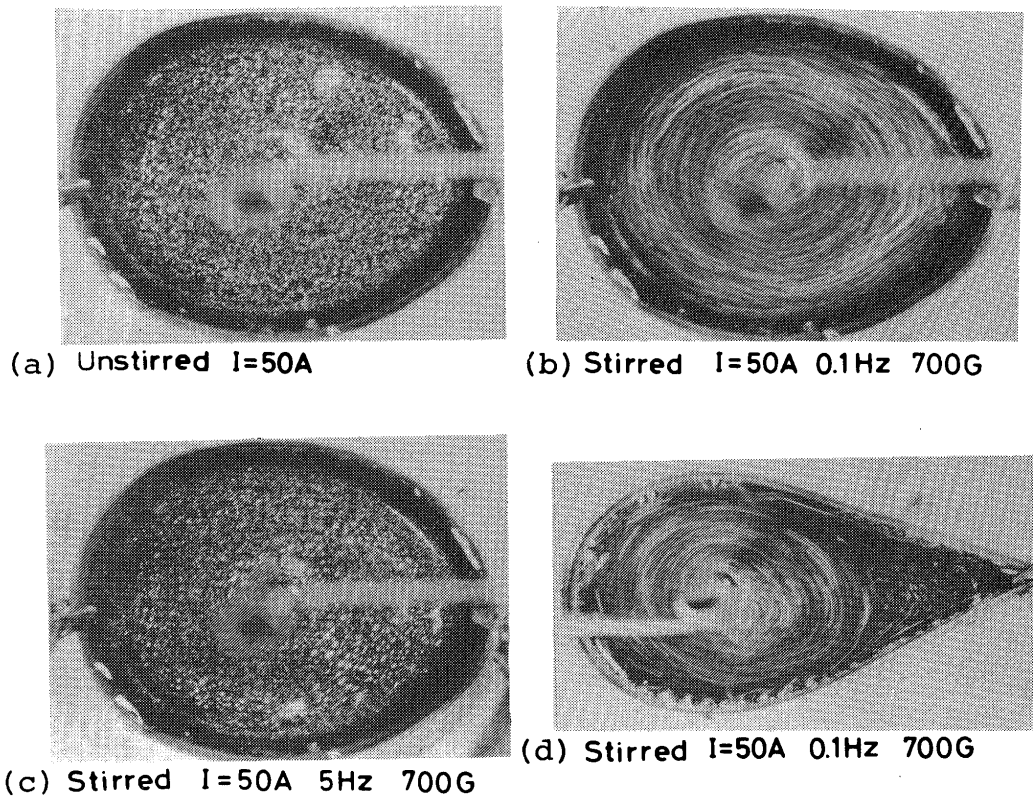


Fig. 16 Surface flow pattern in mercury bath

are about  $10^{\circ}\text{C}$  for 1100 and 1050, about  $60^{\circ}\text{C}$  for 5052 and 5083, about  $130^{\circ}\text{C}$  for 2017 and 2024 and about  $30^{\circ}\text{C}$  for 7N01. Therefore, the susceptibility of the grain refinement is not well explained by the width of solidification range. Another factors due to the difference in a alloy system, such as the difference in the micro morphology of the cellular dendrite during solidification also seems to affect to the susceptibility of the grain refinement. Moreover, from the experimental results in Fig. 15 and in 7N01, it is considered that the grain refining element such as Ti or Zr improves the susceptibility of the grain refinement of 7N01, 5052 (E) and 5083 (J). Further investigation will be continued in future.

### 3.1.8 Sham experiment for electromagnetic stirring by using mercury bath

A sham experiment by using a mercury bath has been carried out in order to qualitatively make clear the flow pattern of the weld puddle. Fig. 16 shows the flow patterns of mercury with and without electromagnetic stirring. The exposure time of filming was decided to be equal to the half cycle of the frequency of the magnetic field so as to observe the flow pattern during the half cycle of the frequency.

In Fig. 16(a) without electromagnetic stirring, the movement of mercury was not observed. In Fig. 16

(b) stirred with the magnetic field of 0.1 Hz and 700 G, mercury was remarkably turned. However with an increasing the frequency from 0.1 to 5 Hz, the flow has been no more observed and it has only slightly been vibrated as shown in Fig. 16(c). Moreover, in Fig. 16(d) where the shape of the mercury bath is imitated to the teardrop of the weld puddle in high welding speed, the flow near the trainling end of the weld puddle is little, though the condition of the magnetic field is equal to that in Fig. 16(b). From these results, it is considered that the effects of the factors mentioned in 3.1 on the grain refinement have been qualitatively explained, though the physical contents of the molten aluminum alloys are different from those of mercury.

### 3.2 Effect of electromagnetic stirring on formation of porosity

As an another effect of the electromagnetic stirring, it is well known that the porosities are decreased in their amount by the electromangetic stirring<sup>10)</sup>. Therefore, the most effective condition of the electromagnetic stirring for elimination of porosities has been also examined. The bead-on-plate welding by the GTA has been carried out with a mixing gas of  $\text{Ar} + 2\%\text{H}_2$  as a shielding gas for 5083 (I).

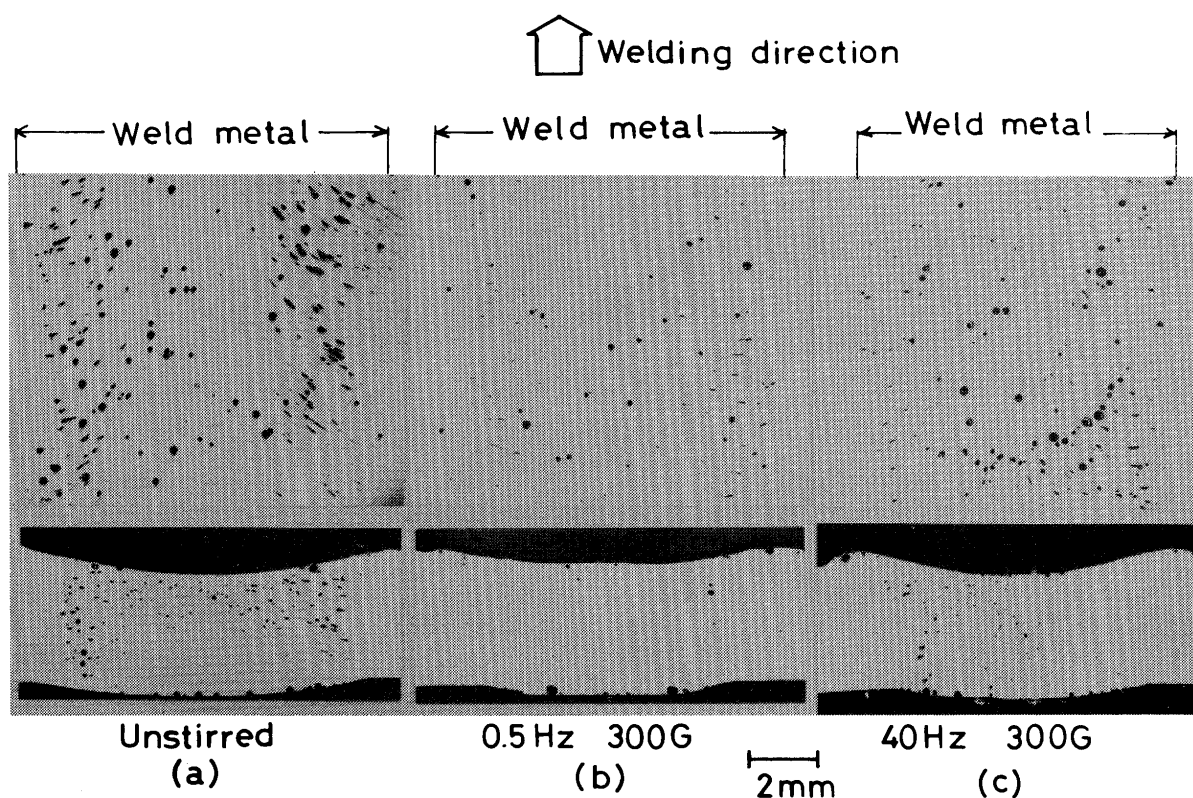


Fig. 17 Effect of electromagnetic stirring on porosity. material;  
5083(I),  $V=130$  mm/min,  $I=100$  A

In Fig. 17, the distributions of the porosities are shown for example in the transverse cross section and also in the parallel surface to the plate surface without and with the electromagnetic stirrings of 0.5 and 40 Hz for 300 G. As a result, without the stirring, a large amount of the porosities were formed. With the stirring induced by the magnetic field of 0.5 Hz and 300 G, the amount of them were remarkably decreased, but in case of 40 Hz and 300 G, the effect of electromagnetic stirring was little. In order to quantitatively evaluate the effect of the frequency of the magnetic field, the area fraction of porosities has been measured on a bead surface after elimination about  $300\ \mu$  in thickness from a weld top surface because the distribution of the porosities was not always uniform in the weld bead, and then the number of cross points in the porosities was measured by using an optical microscope with an eyepiece with 400 points of an intersection mesh. The results are shown in Fig. 18 where the vertical axis indicates an average area fractions of the porosities measured near the fusion boundaries, the weld center and middle part between them. In Fig. 18, it is apparent that the amount of the porosities is the least in the frequencies from 0.5 to 5 Hz. However, the effect of the electromagnetic stirring becomes less effective in the case more than 10

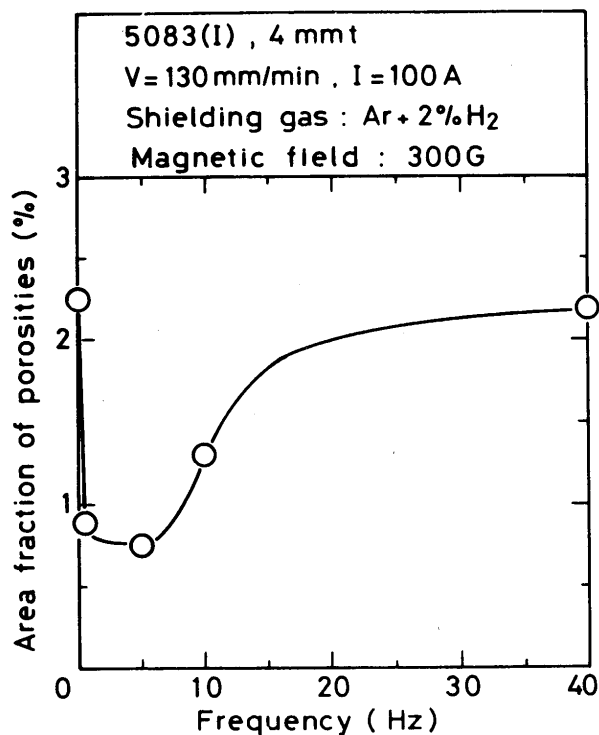


Fig. 18 Relation between frequency of magnetic field and area fraction of porosities



Hz. In addition, as regards to the intensity of the magnetic field, the intensity from 300 to 500 G seems to be the most effective to decrease the amount of porosities as shown in Fig. 19.

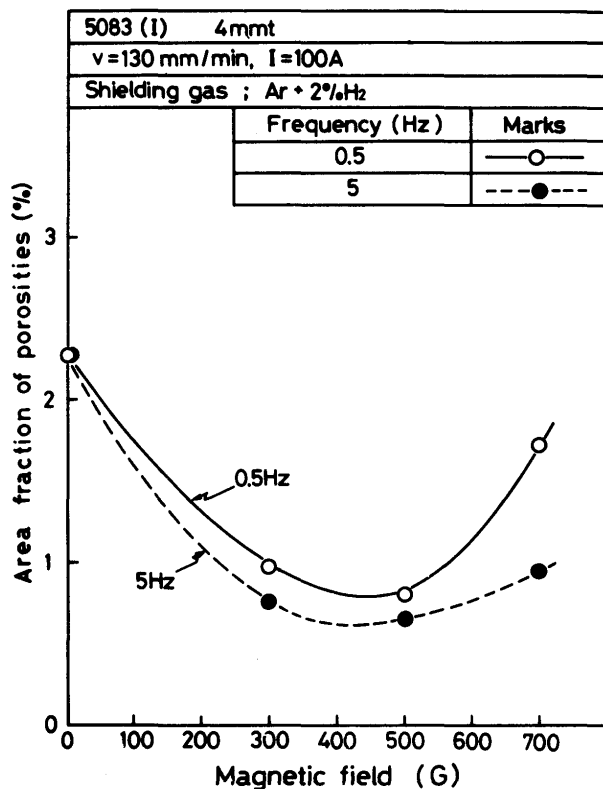


Fig. 19 Relation between intensity of magnetic field and area fraction of porosities

### 3.3 Effect of electromagnetic stirring on formation of feathery crystal

Since a feathery crystal, which is frequently formed in the weld metal of aluminum alloy, lowers the elongation of the weld joint, the formation of the feathery crystal should be avoided. However, it is well known for some aluminum alloys that it is difficult to avoid in the weld center the formation of the feathery crystal using conventional GTA welding process. Therefore, the electromagnetic stirring is considered to be an effective method to avoid the formation of it.

A typical example for the effect of the electromagnetic stirring is shown in Fig. 20 as a combination photograph which shows the change in the structure at a ripple line when the magnetic field is applied. The feathery crystal was growing from left side of it in the weld center, but its growth was completely stopped on the ripple line where the magnetic field was applied. In addition, the relation between the frequency or the intensity of the magnetic field and

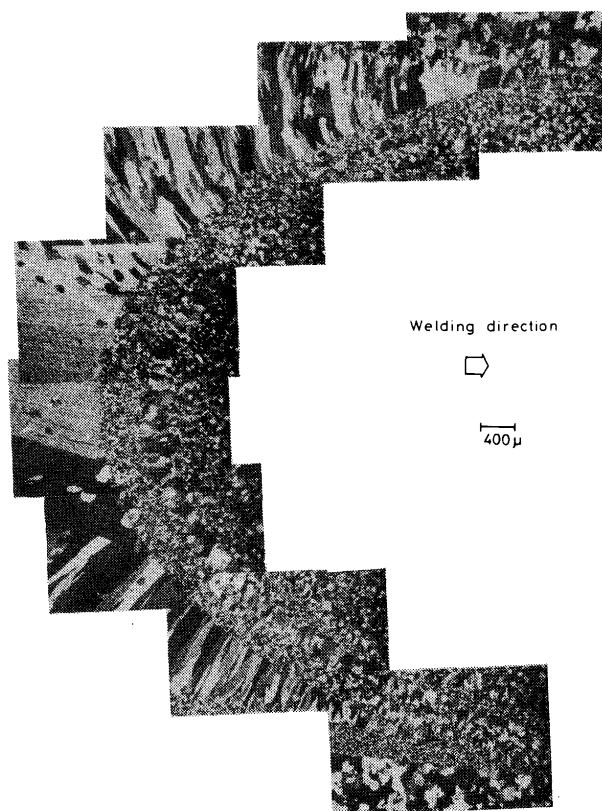


Fig. 20 Extinction of feathery crystal by application of electromagnetic stirring. material; 7N01(K),  $V=250 \text{ mm/min}$ ,  $I=90\text{A}$ , 5 Hz, 300G

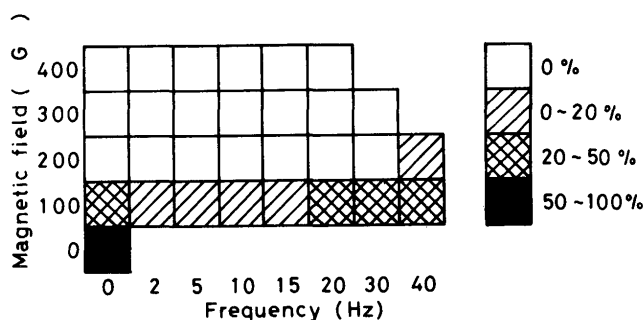


Fig. 21 Composite effect of frequency and intensity of magnetic field on formation of feathery crystal. material; 5052(E),  $V=250 \text{ mm/min}$ ,  $I=70\text{A}$

the formation of the feathery crystal is quantitatively shown in Fig. 21 for 5052 (E). In Fig. 21, the ratio in percent of the length of the feathery crystal to that of the weld bead is shown as the density of hatching. As regards to the effect of the frequency in a constant intensity of 100 G, the feathery crystal has been decreased to 20 to 50% with an unidirectional magnetic field, though there was the ratio of 50 to 100% without magnetic field. Moreover, with 2 to 15 Hz, it has been remarkably decreased to 0 to 20%, but it has been again increased to 20 to 50% with 15 to 40

Hz. Consequently, it is considered that there is an optimum range in frequency to avoid the formation of the feathery crystal as well as the grain refinement. Moreover, the formation of the feathery crystal was also completely eliminated by the magnetic field whose intensity was more than 200 G except 40 Hz. This optimum range was much wider than that for the grain refinement.

### 3.4 Effect of electromagnetic stirring on homogeneity of compositions in weld metal

A homogeneity of the compositions in the weld metal will be also expectable as another effect of the electromagnetic stirring. Fig. 22 and 23 show the typical examples of its effect on a distribution of copper concentration in a butt welded joint between

1100 (B) and 2024 (D) examined by EPMA. In Fig. 22, where distribution of the copper concentration perpendicular to welding direction is shown, the distribution of it undulated in the weld metal without the magnetic stirring as shown in Fig. 22(a) but became considerably uniform by the electromagnetic stirring in the condition of 2 Hz and 300 G as shown in Fig. 22(b). Next, Fig. 23 shows the distribution along the welding direction in the weld center. From Fig. 23(a), without electromagnetic stirring, it has also the undulation pattern which is mainly due to the ripple segregation. On the contrary, it considerably became uniform with magnetic field of 2 Hz and 300 G. Moreover, as the results of the additional examinations with changing the frequency and intensity of the magnetic field, it has been cleared that the homogeneity of the copper concentration was accomplished in the wide range of the magnetic field condition.

### 4. Conclusions

The main conclusions obtained in this investigation for the effect of the electromagnetic stirring in the GTA welding of aluminum alloy sheet are as follows; (1) There is an optimum frequency in alternate magnetic field for the performance of the grain refinement. The optimum frequency is nearly proportional to the welding speed.

(2) The intense magnetic field is effective to the grain refinement, but there is an upper limit for thin sheet owing to the formation of a burnt-through bead.

(3) The grain refinement is remarkable in the welding condition where the structure in the weld metal is almost composed of the columnar crystal without the magnetic field. Therefore, at a high welding speed where the equiaxed crystal zone is formed in the weld center, the effect of the magnetic field is little.

(4) The location of electric ground affect on the degree of the grain refinement and was effective when it was located at the specimen behind and/or forward the weld puddle.

(5) As an observation of the microstructure, the grain refinement has been performed when the growing length of the columnar crystal along the weld center was almost identical to the distance corresponding to the width of the columnar crystal during a half cycle of the alternate magnetic field. This is the reason why the optimum frequency is proportional to the welding speed.

(6) The effect of the grain refinement is largely depended on compositions of materials. 7N01 was the most susceptible to the grain refinement. One each

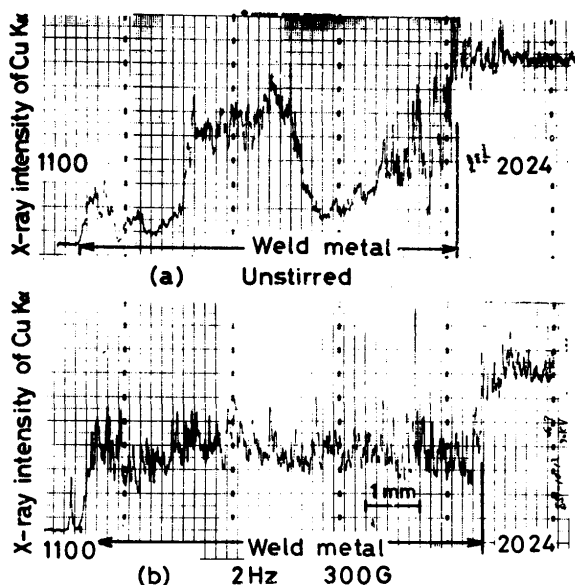


Fig. 22 Effect of electromagnetic stirring on copper distribution in transverse direction to weld line. material; 1100(B) and 2024(D),  $V=250$  mm/min,  $I=70$  A

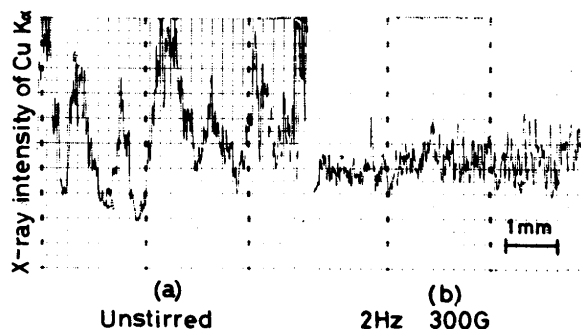


Fig. 23 Effect of electromagnetic stirring on copper distribution along weld center. material; 1100(B) and 2024(D),  $V=250$  mm/min,  $I=70$  A

type of 5052 or 5083 in which weld metal a number of small stray crystals were formed without magnetic field was considerably susceptible, but another one in which weld metal the large columnar crystals were formed was considerably difficult to the refinement. The difference between them is considered to be the difference in their Ti content.

(7) 2017 and 2024 were a little difficult to the grain refinement. 1100 and 1050 were impossible to be refined in this investigation.

(8) The magnetic stirring is effective to reduce the formation of porosities, but there is an optimum condition for the frequency and the intensity of the magnetic field. The excess intensity and/or frequency of the magnetic field decreases its effect.

(9) The magnetic stirring is effective to eliminate the formation of the feathery crystal. There is also optimum condition for the frequency and the intensity of the magnetic field, but the range of the optimum is wider than that of the grain refinement.

(10) The magnetic stirring is effective to homogenize the composition in the weld metal.

#### Acknowledgement

The authors would like to thank Nippon Light Metal Research Laboratory, Ltd. and Kawasaki Heavy Industries, Ltd., for their supplying materials used and chemical analysis.

The authors wish to thank Dr. Masao Ushio, associate professor of JWRI, for his kind suggestions and discussions.

#### References

- 1) T. Fukui: J. Inst. Light Metals, Vol. 25 (1975), No. 3, pp. 88-95 (in Japanese).
- 2) I. Hagiwara, T. Takahasi: J. Inst. Metals, Vol. 29 (1965), No. 6, pp. 637-642 (in Japanese).
- 3) T. Takahasi, I. Hagiwara: J. Inst. Metals, Vol. 29 (1965), No. 12, pp. 1152-1159 (in Japanese).
- 4) W.C. Johnston, G.R. Kotler, S.O'Hara, H.V. Ashcom and W.A. Tiller: Trans. AIME, Vol. 233 (1965), p. 1856.
- 5) S. O'Hara and W.A. Tiller: Trans. AIME, Vol. 239 (1967), pp. 479-501.
- 6) A. Nishimura and U. Kawano: J. Inst. Light Metals, Vol. 25 (1975), No. 6, pp. 193-199 (in Japanese).
- 7) T. Momono and K. Ikawa: J. Inst. Light Metals, Vol. 25 (1975), No. 11, pp. 403-412 (in Japanese).
- 8) D.H. Lane, J.W. Cunningham and W.A. Tiller: Trans. AIME, Vol. 218 (1960), p. 985.
- 9) Y. Onodera: J. Inst. Metals, Vol. 29 (1965), No. 1, pp. 69-73 (in Japanese).
- 10) D.C. Brown, F.A. Crossley, J.F. Rudy and H. Schwartzart: Weld. J., Vol. 41 (1962), 241s.
- 11) V.A. Blinkov: Svar. Proiz., 1975, No. 11, pp. 11-12.
- 12) H. Shibata and K. Asai: Preprints of the National Meeting of JWS, No. 10 (1972), p. 231 (in Japanese).
- 13) H. Shibata and K. Asai: J. JWS, Vol. 41 (1972), No. 7, pp. 811-817 (in Japanese).
- 14) T. Senda, F. Mastuda, M. Kato and H. Nakagawa: J. JWS, Vol. 39 (1970), No. 11, pp. 1180-1189 (in Japanese).
- 15) T. Senda, F. Mastuda, M. Kato and H. Nakagawa: J. JWS, Vol. 40 (1971), No. 3, pp. 242-250 (in Japanese).
- 16) T. Senda, F. Mastuda, M. Kato and H. Nakagawa: J. JWS, Vol. 41 (1972), No. 1, pp. 75-82 (in Japanese).
- 17) ASM: Metals Handbook, 8th edition, Vol. 1 (1961).
- 18) Kobe Steel Ltd.: "Aluminium and Its Alloys" (in Japanese).
- 19) M.F. Jordan and M.C. Coleman: Brit. Weld. J., Vol. 15 (1968), pp. 553-558.
- 20) T. Senda, F. Mastuda, H. Nakagawa, S. Iijima and M. Kato: J. JWS, Vol. 41 (1972), No. 10, pp. 1217-1226 (in Japanese).